communications biology

Article

https://doi.org/10.1038/s42003-024-07428-3

CAF-EVs carry lncRNA MAPKAPK5-AS1 into hepatocellular carcinoma cells and promote malignant cell proliferation

Lin Sheng[1,6], Junmei Lin[2,6], Yili Zhang[3], Yanping Chen[4], Xuxing Ye[2] & Xiaobo Wang[5]

Hepatocellular carcinoma (HCC) is an aggressive malignancy with poor prognosis. LncRNA *MAPKAPK5-AS1* is a potential oncogene and contributes to HCC cell malignant proliferation. This study explores the role of *MAPKAPK5-AS1* carried by carcinoma-associated fibroblasts-derived extracellular vesicles (CAF-EVs) in HCC cell proliferation. Our findings reveal that CAF-EVs promotes HCC cell proliferation by delivering *MAPKAPK5-AS1*, which binds to and inhibits SMURF2 and stabilizes TCF12. SMURF2 leads to TCF12 ubiquitination and degradation. TCF12 upregulates *FOXH1* expression. In animal model, CAF-EVs enhances tumor growth by stabilizing TCF12 via *MAPKAPK5-AS1* and activating *FOXH1* transcription. In conclusion, CAF-EVs carrying *MAPKAPK5-AS1* stabilizes TCF12 expression by competitively inhibiting SMURF2, thus promoting TCF12-mediated *FOXH1* transcription and driving HCC cell proliferation. Our findings may offer insights for HCC treatment and suggest potential targets for future treatments, opening avenues for HCC therapies.

Hepatocellular carcinoma (HCC) is the fifth most prevalent cancer globally and arises from hepatocytes. Its pathogenesis involves multiple processes such as dysregulation of the cell cycle, alterations in DNA methylation, immune modulation, and epithelial-mesenchymal transition (EMT)[1]. Persistent liver inflammation, fibrosis, and cirrhosis are key contributors to the development of HCC[2]. Current therapeutic options for HCC include surgical resection, liver transplantation, percutaneous local ablation, transarterial embolization, and radiotherapy[3]. While targeted therapies have emerged as promising treatments for HCC[4], their efficacy remains under investigation.

Cancer-associated fibroblasts (CAFs) are persistently activated fibroblasts that originate from various sources, including resident fibroblasts within the tumor, hepatic stellate cells, and even HCC cells[5]. Hepatic CAFs are typically characterized by the expression of markers such as smooth muscle α-actin (α-SMA) and fibroblast activation protein α (FAP)[6]. Extracellular vesicles (EVs), a diverse group of membrane-bound vesicles derived from the nuclear envelope or plasma membrane, play a significant role in intercellular communication and regulation of cellular processes[7].

The interaction between CAF and EVs is crucial in shaping the tumor microenvironment (TME), facilitating crosstalk between malignant and non-malignant components of the TME[8]. Emerging evidence suggests that CAF-EVs can deliver both pro- and anti-tumor molecules that influence the progression of HCC[9,10]. In this study, we investigated the mechanism through which CAF-EVs promote the malignant behavior of HCC cells by exploring their role in tumor cell proliferation and identifying potential molecular targets for therapeutic intervention.

Long non-coding RNAs (lncRNAs), a class of RNA transcripts >200 nucleotides, play a pivotal role in regulating gene expression through mechanisms such as chromatin remodeling and histone modification[11]. Extensive research has demonstrated that lncRNAs are implicated in the development and progression of various cancers, including HCC[12–16]. One such lncRNA, *MAPKAPK5-AS1*, has recently been identified as being significantly upregulated in HCC tissues. *MAPKAPK5-AS1* has been shown to promote HCC cell proliferation, migration, invasiveness, and EMT, contributing to tumor progression and poor prognosis[17–19]. Interestingly, CAF-EVs are known to carry lncRNAs that participate in cancer progression[20], but the role of *MAPKAPK5-AS1* carried by CAF-EVs in HCC remains unexplored.

SMAD-specific E3 ubiquitin protein ligase 2 (SMURF2) is a homologous to the E6-associated protein C-terminus-type E3 ubiquitin ligase and is critical for modulating the stability of Smad proteins. It plays a significant role in processes such as tumor metastasis, cell apoptosis, and cell cycle

[1]The department of internal medicine, Jinhua Municipal Central Hospital, Jinhua, China. [2]Department of Traditional Chinese Medicine, Jinhua Municipal Central Hospital, Jinhua, China. [3]Department of Health Management Center, Affiliated Jinhua Hospital, Zhejiang University School of Medicine, Jinhua, China. [4]Department of Gastroenterology, Jinhua Municipal Central Hospital, Jinhua, China. [5]The Fourth School of Clinical Medicine, Zhejiang Chinese Medical University, Hangzhou, China. [6]These authors contributed equally: Lin Sheng, Junmei Lin. e-mail: wangxiaobo2120@163.com

regulation[21]. SMURF2 has been identified as a potent tumor suppressor in several cancers[22], including lung[23] and ovarian cancer[24]. In HCC, SMURF2 overexpression has been shown to inhibit cell migration and tumor metastasis[25]. Based on this, we hypothesize that lncRNA *MAPKAPK5-AS1* may competitively bind to SMURF2, thereby stabilizing key transcription factor proteins.

Transcription factor 12 (TCF12), a member of the basic helix-loop-helix E protein family, is expressed in various tissues, including skeletal muscle, thymus, and immune cells[26]. TCF12 is often implicated as an oncogenic factor; its overexpression has been observed in ovarian cancer and HCC, where it promotes cell proliferation and drives the cell cycle from the G0/G1 phase to the S phase[27,28]. Additionally, TCF12 has been associated with EMT, contributing to tumor growth and metastasis[29]. This study aims to further elucidate the regulatory mechanisms of TCF12 in HCC.

Forkhead box (FOX) family proteins are key regulatory factors of embryonic development, physiological processes, and cellular homeostasis[30]. Several FOX proteins, including FOXM1, FOXO, and FOXH1, are involved in cancer progression, drug resistance, and metastasis[31–33]. Of particular interest is FOXH1, which is overexpressed in lung cancer and HCC tissues. It plays a critical role in EMT, cancer progression and metastasis[34,35]. Knockdown of FOXH1 has been shown to significantly inhibit cancer cell growth, invasion, and induce cell death[32]. In HCC, FOXH1 overexpression enhances colony formation, migration, and invasion of tumor cells[36].

In this study, we demonstrate that CAF-EVs promote malignant proliferation in HCC cells by disrupting the inhibitory effects of SMURF2 on TCF12/*FOXH1* via the delivery of *MAPKAPK5-AS1*. These findings offer insights into potential therapeutic strategies for treating HCC.

Results

Isolation, Culture, and Extraction of CAFs and EVs

We successfully isolated and cultured CAFs from HCC patient tissues, and normal fibroblasts (NFs) from adjacent normal tissues. Immunofluorescence staining confirmed that NFs and CAFs were negative for keratin and CD31 (endothelial cell marker) and positive for Vimentin. Notably, NFs exhibited negative expression of α-SMA, while CAFs were positive for α-SMA (Fig. 1A), confirming the typical phenotypes of NFs and CAFs, and the isolated cells were free from contamination with endothelial cells. EVs were subsequently extracted from both NFs and CAFs. Transmission electron microscopy (TEM) revealed characteristic cup-shaped structures in both NF-EVs and CAF-EVs (Fig. 1B). Nanoparticle tracking analysis (NTA) analysis determined the concentration of NF-EVs to be 9.3×10^6 particles per mL and CAF-EVs to be 1.3×10^7 particles per mL (Fig. 1C). Western blot analysis of EV marker proteins showed positive expression of CD9 and CD63 in both NF-EVs and CAF-EVs, while Calnexin was absent, consistent with the positive control (Fig. 1D). These findings confirm the successful isolation and characterization of both NF-EVs and CAF-EVs.

CAF-EVs promote malignant proliferation of HCC Cells

Huh-7 and HCC36 cells were co-cultured with NF-EVs and CAF-EVs, each containing 100 μg of total protein. The cell counting kit (CCK)-8 assay demonstrated a significant increase in cell viability following co-culture with CAF-EVs compared to the control ($p < 0.01$, Fig. 2A). Western blot analysis further showed a marked upregulation of the proliferation marker proliferating cell nuclear antigen (PCNA) in HCC cells treated with CAF-EVs ($p < 0.01$, Fig. 2B). Additionally, the 5-Ethynyl-2'-Deoxyuridine (EdU) assay and colony formation assay revealed significantly enhanced cell proliferation ability in the presence of CAF-EVs ($p < 0.01$, Fig. 2C, D). Collectively, these findings indicate that CAF-EVs significantly promote the malignant proliferation of HCC cells.

CAF-EVs transport *MAPKAPK5-AS1* into HCC cells

Previous research has demonstrated that *MAPKAPK5-AS1* is overexpressed in HCC[37] and can be transferred into HCC cells via EVs, promoting cell proliferation[38]. Based on this, we hypothesized that CAF-EVs may carry *MAPKAPK5-AS1* and influence the proliferation of HCC

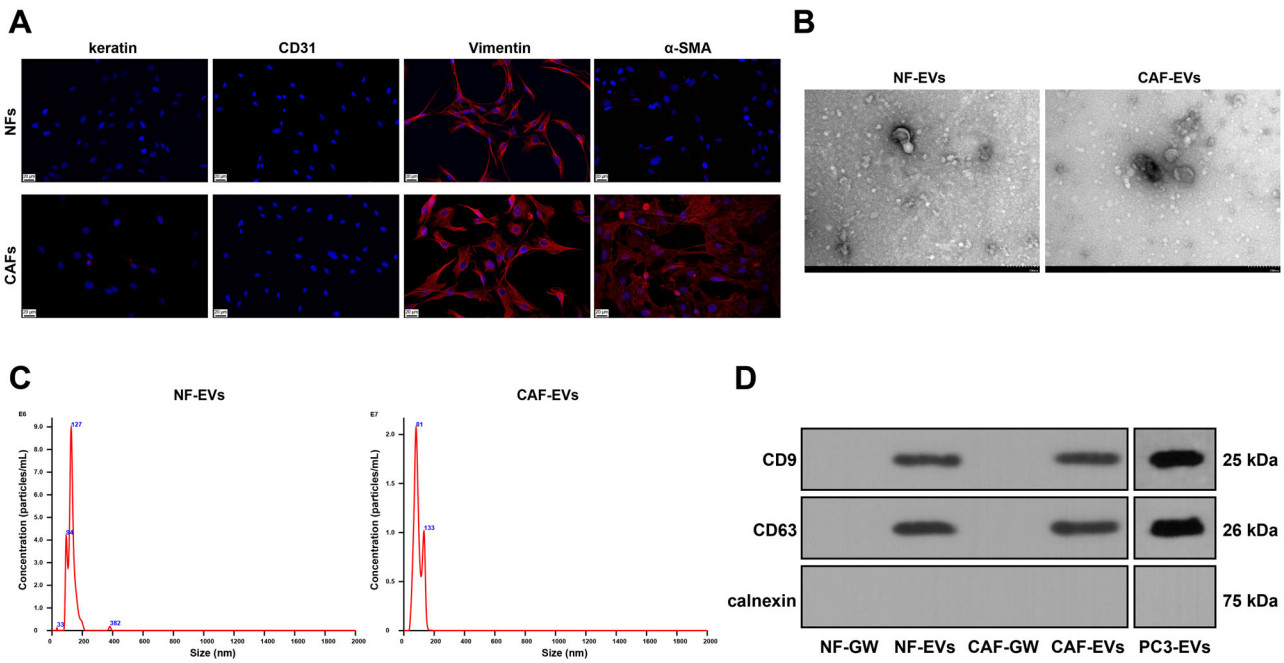

Fig. 1 | Isolation, culture, and extraction of CAFs and EVs. NFs and CAFs, as well as their EVs, were isolated. **A** Immunofluorescence staining was performed to detect the expression of Vimentin, CD31, fibronectin, and α-SMA. **B** Morphological observations of NF-EVs and CAF-EVs were conducted under TEM. **C** The concentration and particle size of NF-EVs and CAF-EVs were measured using NTA. **D** Western blot assay was performed to examine the expression of surface markers CD9, CD63, and calnexin on NF-EVs and CAF-EVs. $N = 3$ independent biological replicates. CAF Cancer-associated fibroblast, EVs extracellular vesicles, NF normal fibroblasts, α-SMA smooth muscle α-actin, GW GW4869, PC3-EVs positive control.

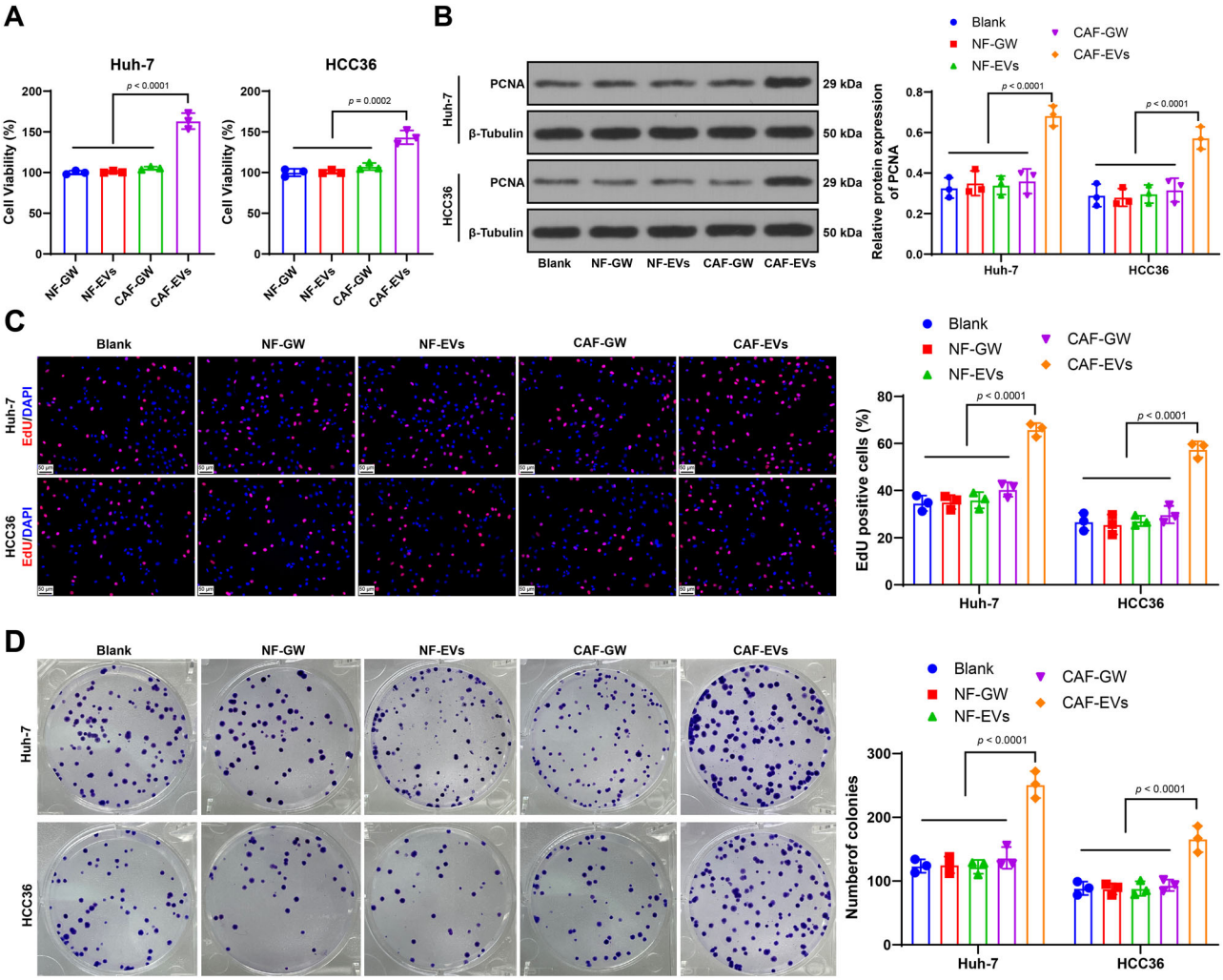

Fig. 2 | CAF-EVs promote malignant proliferation of HCC cells. Huh-7 or HCC36 cells were treated with NF-EVs or CAF-EVs containing 100 μg of total protein, with NF-GW and CAF-GW treatment as negative controls. **A** Cell proliferation ability was assessed using the CCK-8 assay. **B** PCNA expression was examined by Western blot assay. **C** Cell proliferation was detected using EdU staining. **D** Colony formation assay was performed to assess cell proliferation ability. Data are presented as mean ± standard deviation ($N = 3$ independent biological replicates). $^{**}p < 0.01$. Data in (**A**) was conducted using one-way ANOVA, while data in (**B**–**D**) were analyzed using two-way ANOVA, followed by Tukey's multiple comparisons test. CAF Cancer-associated fibroblast, EVs extracellular vesicles, NF normal fibroblasts, PCNA proliferating cell nuclear antigen, GW GW4869. Error bars represent the standard deviation.

cells. Quantitative real-time polymerase chain reaction (qRT-PCR) results revealed significantly higher levels of *MAPKAPK5-AS1* in CAFs and CAF-EVs than in NFs and NF-EVs ($p < 0.01$, Fig. 3A). Treatment with RNase A did not affect the expression of *MAPKAPK5-AS1* in CAF-EVs, whereas Triton X-100 treatment significantly reduced its expression ($p < 0.01$, Fig. 3B), confirming that *MAPKAPK5-AS1* is encapsulated within CAF-EVs. To further confirm this, cy3-labeled *MAPKAPK5-AS1* was transfected into CAFs, which were then co-cultured with Huh-7 or HCC36 cells labeled with fluorescein isothiocyanate (FITC)-phalloidin. Red fluorescence was observed in the recipient cells, but was absent when GW4869 (an inhibitor of EV release) was applied ($p < 0.01$, Fig. 3D). Moreover, *MAPKAPK5-AS1* expression in Huh-7 and HCC36 cells was significantly upregulated after CAF-EVs treatment ($p < 0.01$, Fig. 3C). Collectively, these findings confirm that CAF-EVs transport *MAPKAPK5-AS1* into HCC cells.

Overexpression of *MAPKAPK5-AS1* in CAF-EVs enhances malignant proliferation of HCC cells

To further elucidate the role of *MAPKAPK5-AS1* in promoting HCC proliferation, we overexpressed *MAPKAPK5-AS1* in CAFs ($p < 0.01$, Fig. 4A) and subsequently isolated CAF-EVs with high *MAPKAPK5-AS1* expression (CAF-EVs-AS1) ($p < 0.01$, Fig. 4B). Co-culture of CAF-EVs-AS1 with Huh-7 and HCC36 cells resulted in significantly increased *MAPKAPK5-AS1* levels in the recipient cells ($p < 0.01$, Fig. 4C), along with enhanced cell viability and proliferation ($p < 0.05$, Fig. 4D–G). These findings suggest that the overexpression of *MAPKAPK5-AS1* in CAF-EVs further promotes malignant proliferation of HCC cells, highlighting the role of *MAPKAPK5-AS1* in this process.

MAPKAPK5-AS1 competitively binds to SMURF2 in HCC cells to stabilize TCF12 expression

Previous studies have demonstrated that lncRNAs can stabilize transcription factor proteins by binding to ubiquitin ligases, thereby preventing their ubiquitination and degradation[39]. However, whether *MAPKAPK5-AS1* exerts such a function in HCC cells has not been explored. Since TCF12 is known to be highly expressed in HCC and promotes tumor progression[28], while SMURF2 is downregulated[25], we hypothesized that *MAPKAPK5-AS1* might stabilize TCF12 by competitively binding to SMURF2. RPISeq database analysis revealed that

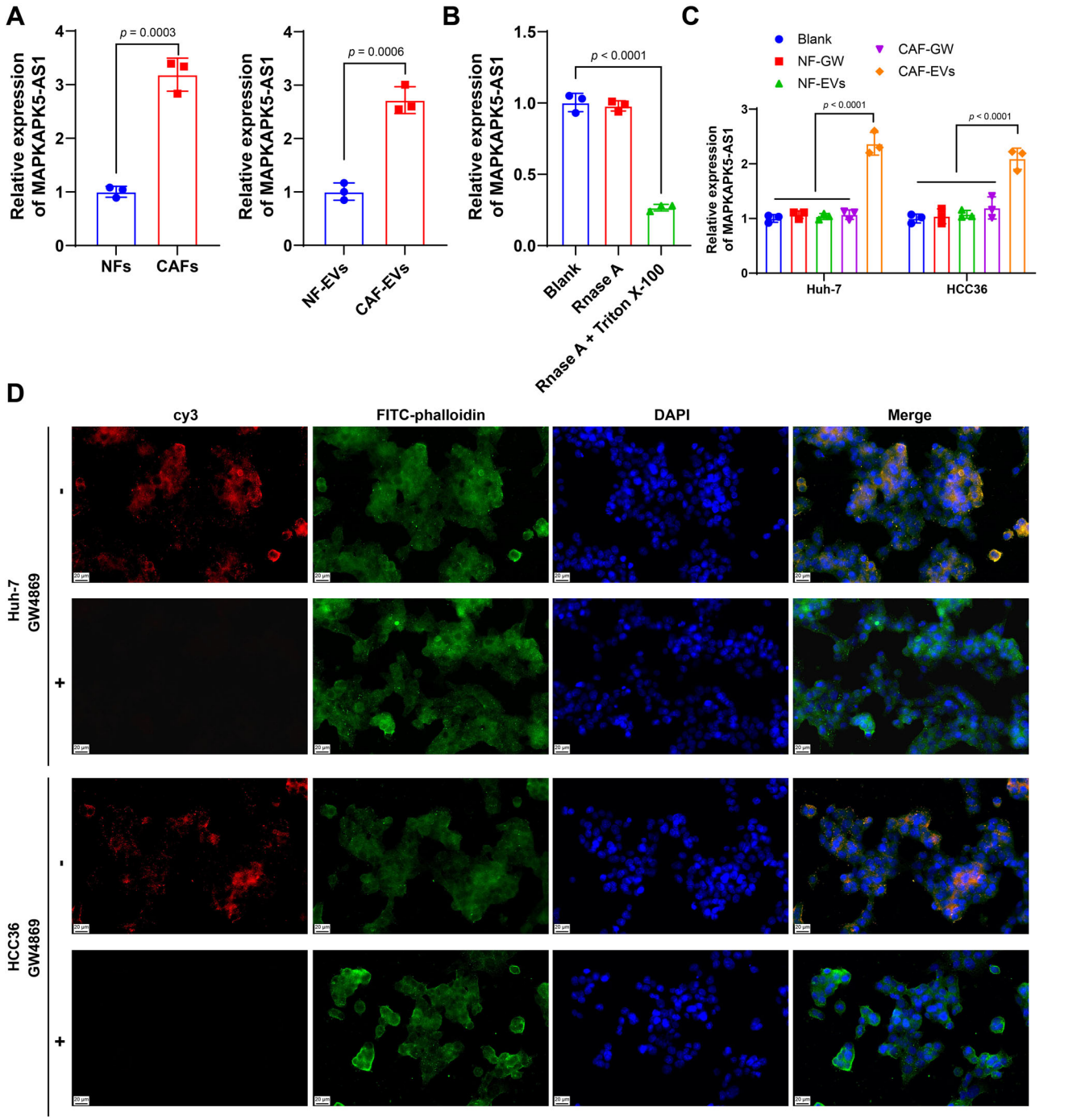

Fig. 3 | CAF-EVs carry *MAPKAPK5-AS1* into HCC cells. A qRT-PCR was performed to measure the *MAPKAPK5-AS1* expression in NFs, CAFs, and isolated NF-EVs and CAF-EVs. **B** After treatment with Rnase A or a combination of Rnase A and Triton X-100, qRT-PCR was used to assess the expression of *MAPKAPK5-AS1* in CAFs. **C** qRT-PCR was used to detect the expression of *MAPKAPK5-AS1* in Huh-7 and HCC36 cells. **D** Confocal microscopy was employed to observe the transfer of cy3-labeled *MAPKAPK5-AS1*. Data are presented as mean ± standard deviation ($N = 3$ independent biological replicates). $^{**}p < 0.01$. Data comparison between two groups in (**A**) was performed using *t*-test, while data comparison in (**B**) was analyzed using one-way ANOVA. Data comparison in (**C**) was analyzed using two-way ANOVA, followed by Tukey's multiple comparisons test. CAF Cancer-associated fibroblast, EVs extracellular vesicles, NF normal fibroblasts.

MAPKAPK5-AS1 can bind to TCF12 (Fig. 5A), and lncATLAS database analysis, supported by subcellular fractionation experiments, confirmed that *MAPKAPK5-AS1* is localized in the cytoplasm ($p < 0.01$, Fig. 5B, C). RNA pull-down experiments confirmed the binding between *MAPKAPK5-AS1* and TCF12 (Fig. 5D). Although treatment with CAF-EVs did not significantly alter *TCF12* mRNA levels ($p > 0.05$, Fig. 5F), it reduced TCF12 ubiquitination (Fig. 5G), and increased TCF12 protein expression ($p < 0.01$, Fig. 5I). Co-IP experiments showed an interaction between TCF12 and SMURF2 (Fig. 5E). Furthermore, *SMURF2* overexpression in Huh-7 and HCC36 cells significantly elevated TCF12 ubiquitination, but this effect was reversed by the proteasome inhibitor MG132 ($p < 0.05$, Fig. 5G–I). These findings demonstrate that *MAPKAPK5-AS1* carried by CAF-EVs competitively binds to SMURF2 in HCC cells, thereby stabilizing TCF12 expression.

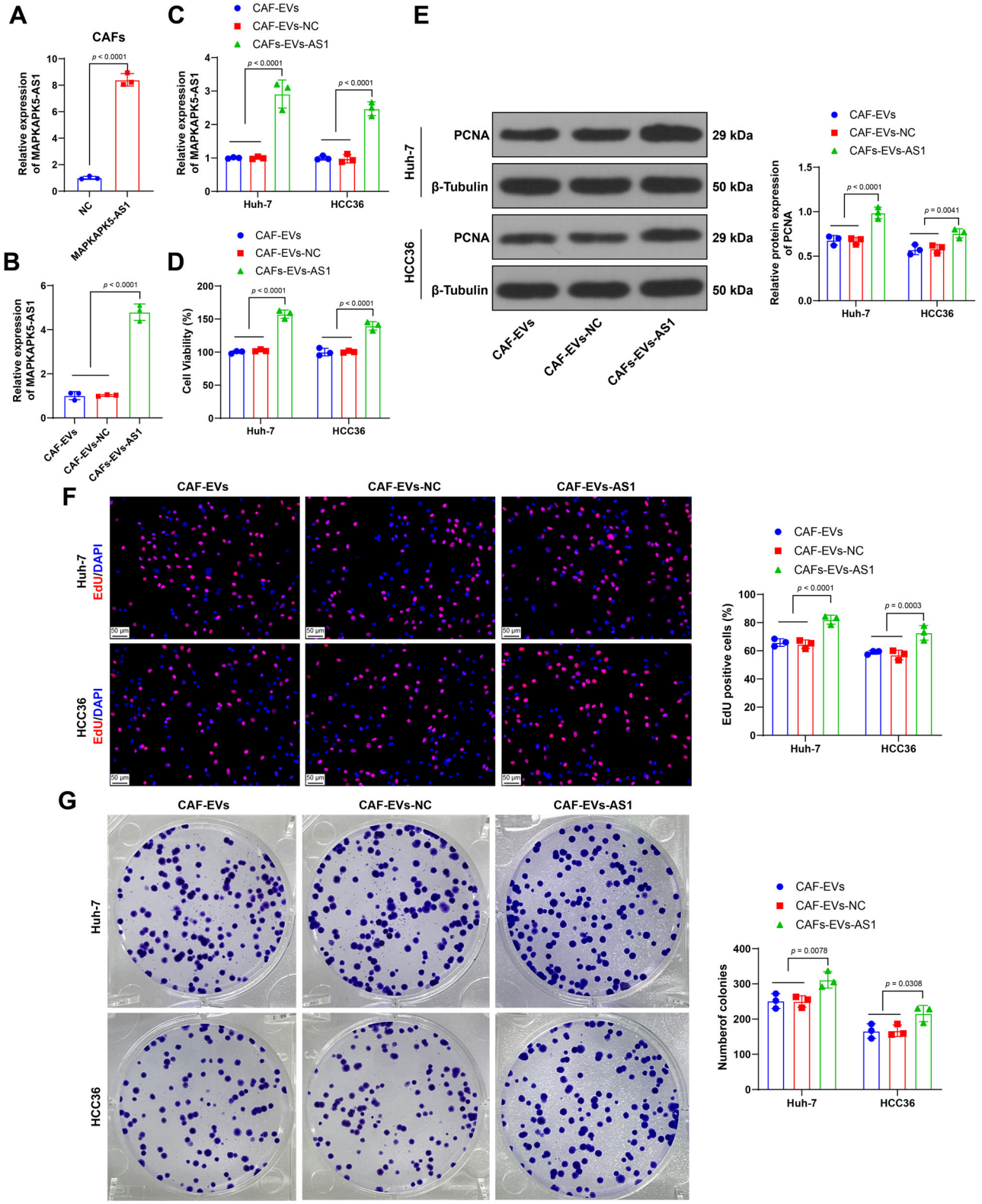

Fig. 4 | Overexpression of *MAPKAPK5-AS1* in CAF-EVs further promotes malignant proliferation of HCC cells. CAFs were infected with a lentiviral overexpression vector of *MAPKAPK5-AS1* (*MAPKAPK5-AS1*), with lentiviral overexpression vector of NC (NC) as a negative control. **A** qRT-PCR was performed to detect the expression of *MAPKAPK5-AS1* in CAFs; subsequently, EVs were isolated and treated with Huh-7 and HCC36 cells. **B** qRT-PCR was used to measure the expression of *MAPKAPK5-AS1* in CAF-EVs. **C** qRT-PCR was used to measure the expression of *MAPKAPK5-AS1* in Huh-7 and HCC36 cells. **D** Cell viability was assessed using the CCK-8 assay. **E** Western blot assay was performed to detect the expression of PCNA. **F** EdU staining was used to assess cell proliferation. **G** Colony formation assay was conducted to evaluate cell proliferation. Data are presented as mean ± standard deviation ($N = 3$ independent biological replicates). $^{*}p < 0.05$, $^{**}p < 0.01$. Data comparisons in (**A**, **B**) were analyzed using *t*-test, while data comparisons in (**C**–**G**) were analyzed using two-way ANOVA, followed by Tukey's multiple comparisons test. CAF Cancer-associated fibroblast, EVs extracellular vesicles, NF normal fibroblasts, PCNA proliferating cell nuclear antigen.

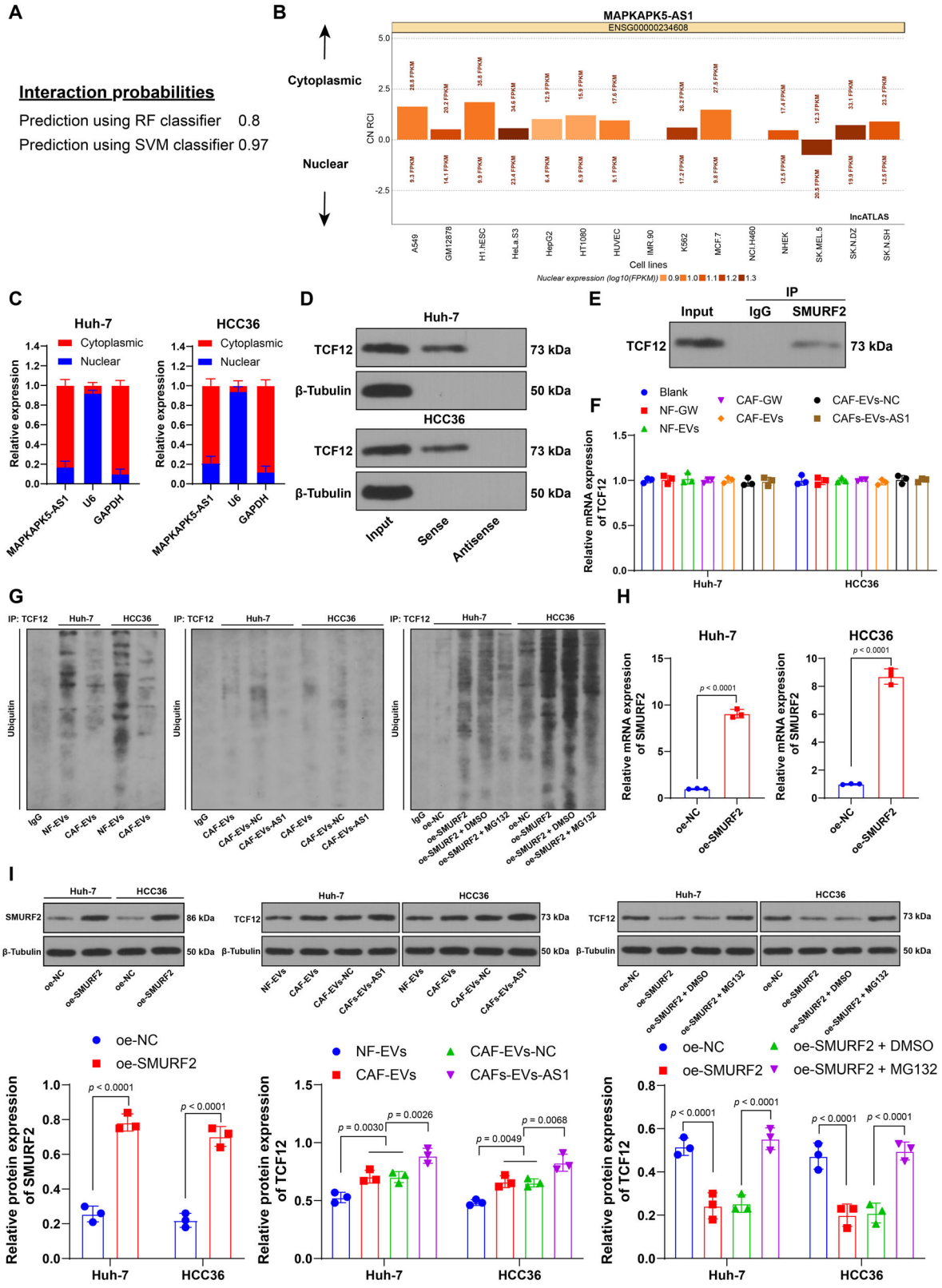

CAF-EVs partially reverse the inhibitory effect of *SMURF2* overexpression on HCC cell proliferation

Next, we investigated whether CAF-EVs could counteract the growth-suppressive effects of *SMURF2* overexpression in HCC cells. Overexpression of *SMURF2* significantly inhibited the proliferation of Huh-7 and HCC36 cells. However, co-culturing with CAF-EVs-AS1 effectively reversed this inhibition, as evidenced by increased cell viability ($p < 0.01$, Fig. 6A), upregulated PCNA expression ($p < 0.01$, Fig. 6B), a higher number of EdU-positive cells ($p < 0.01$, Fig. 6C), and a significant increase in colony formation ($p < 0.01$, Fig. 6D). These findings suggest that CAF-EVs-AS1 can mitigate the inhibitory effects of Smurf2 overexpression on the malignant proliferation of HCC cells.

Fig. 5 | *MAPKAPK5-AS1* competitively binds to SMURF2 in HCC cells to stabilize the expression of TCF12. **A** The binding between *MAPKAPK5-AS1* and TCF12 was analyzed using the RPISeq database. **B** The subcellular localization of *MAPKAPK5-AS1* was analyzed using the lncATLAS database. **C** Subcellular localization of *MAPKAPK5-AS1* was determined using nuclear-cytoplasmic fractionation assay, with U6 and GAPDH as internal controls for the nucleus and cytoplasm, respectively. **D** RNA pull-down assay was performed to detect the binding between *MAPKAPK5-AS1* and TCF12. **E** CoIP assay was conducted to examine the binding between SMURF2 and TCF12. **F** qRT-PCR was used to measure the mRNA levels of *TCF12* in cells treated with different conditions. **G** Ubiquitination assay was performed to assess the ubiquitination levels of TCF12 in cells treated with different conditions. **H** qRT-PCR was conducted to detect the mRNA levels of *SMURF2* in cells transfected with overexpression vector of *SMURF2*, with oe-NC as a control. **I** Western blot assay was performed to analyze the expression of SMURF2 and TCF12 in cells treated with different conditions. Data are presented as mean ± standard deviation ($N = 3$ independent biological replicates). $^{*}p < 0.05$, $^{**}p < 0.01$. Data comparations in (**H**) were analyzed using *t*-test, while data comparations in (**F**, **I**) were analyzed using two-way ANOVA, followed by Tukey's multiple comparisons test. CAF Cancer-associated fibroblast, EVs extracellular vesicles, NF normal fibroblasts, PCNA proliferating cell nuclear antigen, TCF12 Transcription factor 12, SMURF2 SMAD-specific E3 ubiquitin protein ligase 2, GW GW4869.

TCF12 binds to the *FOXH1* promoter and enhances *FOXH1* expression

Using the JASPAR database, we predicted binding sites for TCF12 on the *FOXH1* promoter (Fig. 7A). Given that *FOXH1* is highly expressed in HCC[36], we hypothesized that TCF12 might promote *FOXH1* transcription. Chromatin immunoprecipitation (ChIP) analysis demonstrated significant TCF12 enrichment on the *FOXH1* promoter ($p < 0.01$, Fig. 7B), and the dual-luciferase reporter assay revealed a marked increase in luciferase activity ($p < 0.01$, Fig. 7C). Additionally, qRT-PCR and Western blot assays showed that *SMURF2* overexpression inhibited *FOXH1* expression, but this suppression was reversed by the addition of CAF-EVs or CAF-EVs-AS1 ($p < 0.01$, Fig. 7D–E). These findings indicate that TCF12 binds to the *FOXH1* promoter in HCC cells and enhances its expression in HCC cells.

Suppression of *FOXH1* partially reverses the promotive effect of CAF-EVs on malignant proliferation of HCC cells

To further validate the proposed mechanism, we transfected siRNAs targeting FOXH1 (si-FOXH1) into Huh-7 cells, effectively reducing FOXH1 expression ($p < 0.01$, Fig. 8A, B). Subsequently, we conducted combined experiments using CAF-EVs-AS1 with the two siRNAs that exhibited the most potent inhibitory effects. Compared to treatment with CAF-EVs-AS1 alone, *FOXH1* suppression led to a significant decrease in cell viability ($p < 0.01$, Fig. 8C) and inhibition of cell proliferation ($p < 0.01$, Fig. 8B, D, E). These findings indicate that the promotive effect of CAF-EVs-AS1 on the malignant proliferation of HCC cells is partially reversed when *FOXH1* is suppressed.

CAF-EVs promote HCC growth in vivo

To assess the effects of CAF-EVs in vivo, we established a nude *mouse* xenograft model using Huh-7 cells. Treatment with CAF-EVs and CAF-EVs-AS1 significantly promoted tumor growth, as demonstrated by increased tumor weight and volume ($p < 0.01$, Fig. 9A–C), and a higher percentage of KI67-positive cells in the tumors ($p < 0.01$, Fig. 9D). Furthermore, the expression levels of *MAPKAPK5-AS1*, *TCF12*, and *FOXH1* were markedly elevated in the tumors, whereas SMURF2 expression remained unchanged ($p < 0.01$, Fig. 9E, F). These findings confirm that CAF-EVs promote HCC tumor growth by delivering *MAPKAPK5-AS1*, competitively binding to SMURF2, stabilizing TCF12 expression, and enhancing *FOXH1* expression.

Discussion

The TME of HCC is a highly complex and heterogeneous structure, interacting with various immune cells and their secreted factors[40]. Among these components, CAFs contribute to tumor progression by promoting tumor growth, angiogenesis, invasion, metastasis, extracellular matrix remodeling, and even drug resistance through the secretion of various cytokines[41]. Additionally, CAF-derived factors are known to enhance HCC proliferation and metastasis[42]. In our study, we demonstrated that CAF-EVs enter HCC cells by carrying *MAPKAPK5-AS1*, which competitively binds to SMURF2, stabilizing the expression of TCF12. This stabilization subsequently promotes *FOXH1* expression, thereby facilitating the malignant proliferation of HCC cells (Fig. 10).

CAF and their EVs have been shown to influence multiple aspects of cancer progression, including EMT, invasion, metastasis, stemness, proliferation, growth, and chemoresistance[20]. Upon co-incubation of CAF-EVs with HCC cells, we observed an increase in cell viability and a significant enhancement of proliferative capacity, confirming the role of CAF-EVs in promoting HCC malignancy. CAF-EVs contribute to drug resistance, immune evasion, and the promotion of aggressive cancer phenotypes by carrying various molecular cargo[43]. In line with these findings, our results identified the lncRNA *MAPKAPK5-AS1* as a key factor transported by CAF-EVs that enhances the proliferation and survival of HCC cells.

MAPKAPK5-AS1, a newly discovered lncRNA, is overexpressed in HCC and has been associated with larger tumor size, advanced tumor stages, and increased lymph node metastasis[18,44]. Based on these observations, we propose that CAF-EVs deliver *MAPKAPK5-AS1* into HCC cells, promoting their tumorigenic behavior. Consistent with our findings, *MAPKAPK5-AS1* has been shown to competitively bind to miR-376b-5p, protecting epithelial transition sequence 2 (ECT2) from degradation and promoting HCC cell migration and invasion[19]. Other studies have similarly reported that *MAPKAPK5-AS1* enhances proliferation, invasion, migration, and EMT in HCC cells through a competing endogenous RNA (ceRNA) network[17,18].

LncRNAs, through their competitive endogenous RNA functions, typically operate in the cytoplasm by binding to miRNAs, alleviating their suppressive effects on target gene mRNAs, and consequently influencing gene expression[45]. Collectively, our findings reveal that CAFs-EVs carried *MAPKAPK5-AS1* into HCC cells, enhancing their proliferative capacity. Exploring the downstream mechanisms of *MAPKAPK5-AS1*, particularly its interactions with miRNAs, will be a key focus for future research.

Our study demonstrated that CAF-EVs carrying *MAPKAPK5-AS1* entered HCC cells and competitively bound to SMURF2, stabilizing TCF12 expression. SMURF2 is known for its role in cancer suppression through various pathways. For example, elevated SMURF2 expression inhibits EMT in pancreatic cancer and is negatively associated with gemcitabine resistance[46]. In HCC, SMURF2 promotes the ubiquitination of Smad2 via a proteasome-dependent degradation pathway, thereby reducing EMT[25]. Additionally, *SMURF2* acts as an inhibitor of BMP signaling, enhancing the antitumor effects of Romidepsin against HCC[47]. Interestingly, in contrast, *SMURF2* knockdown has been shown to increase the sensitivity of non-small cell cancer cells to cisplatin and radiotherapy, leading to increased cancer cell apoptosis[48]. These opposing effects of SMURF2 across different cancers suggest that its role is highly context-dependent and warrants further exploration.

In our study, overexpression of *SMURF2* inhibited HCC cell viability, reduced PCNA expression, and decreased EdU-positive cells and colony formation. However, when HCC cells were co-cultured with CAF-EVs carrying high levels of *MAPKAPK5-AS1*, the inhibitory effect of *SMURF2* on malignant cell proliferation was partially reversed. This suggests that CAF-EVs carrying *MAPKAPK5-AS1* can modulate the effects of *SMURF2* in HCC. Moreover, SMURF2 has been shown to inhibit TGF-β signaling and reduce the risk of hepatitis C virus-induced HCC[49], providing an avenue for future investigation into the mechanisms of Smurf2 in HCC.

Next, we examined the role and downstream mechanisms of TCF12 in HCC. TCF12 is a crucial transcription factor involved in cancer progression

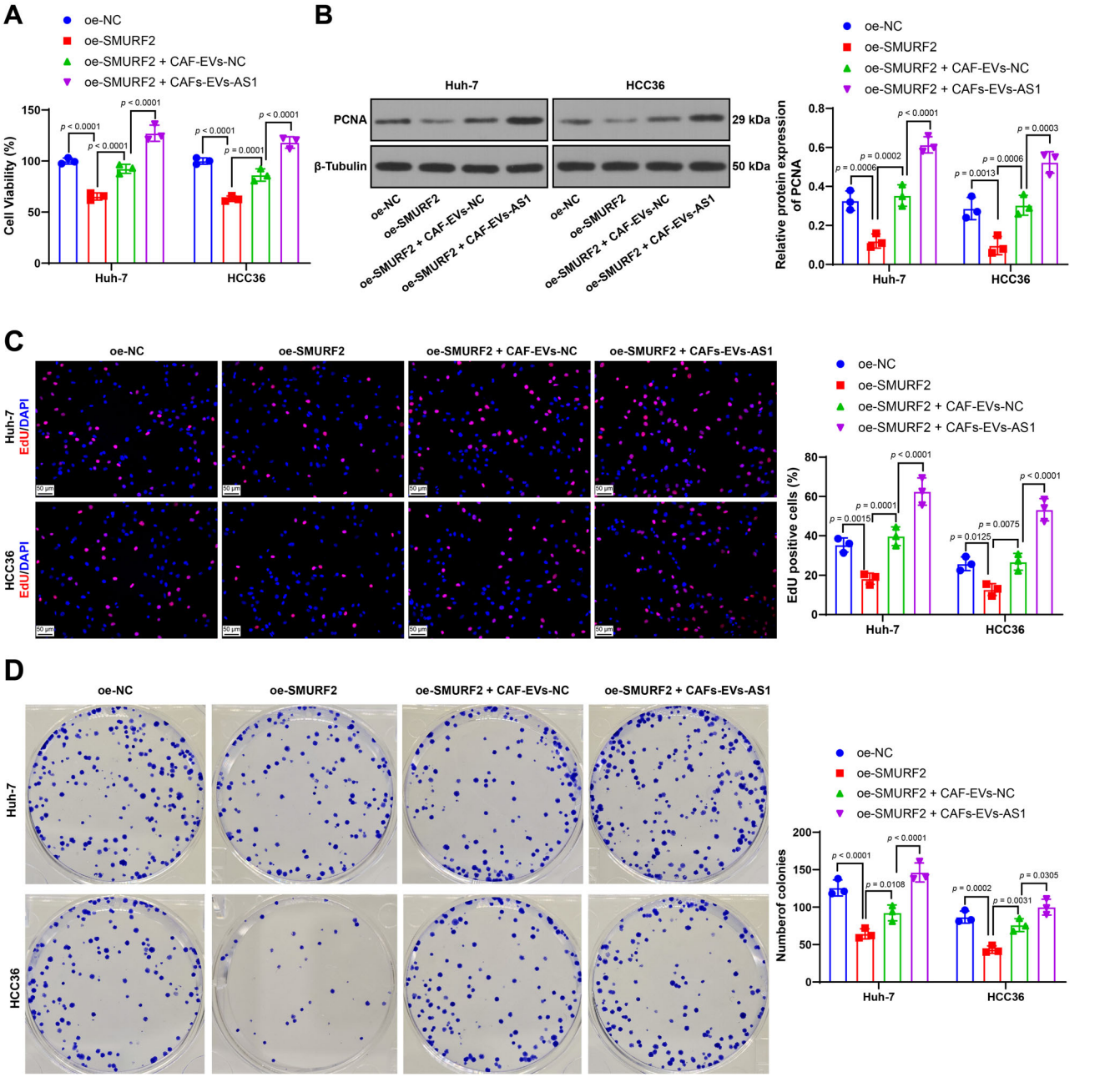

Fig. 6 | CAF-EVs partially reverse the inhibitory effect of *SMURF2* overexpression on malignant proliferation of HCC cells. Huh-7 and HCC36 cells were transfected with the overexpression vector of *SMURF2* (oe-SMURF2), with oe-NC as a control. Subsequently, the cells were treated with CAF-EVs-NC or CAF-EVs-AS1 containing 100 μg of total protein. **A** Cell viability was assessed using the CCK-8 assay. **B** Western blot assay was performed to detect the expression of PCNA. **C** EdU staining was used to assess cell proliferation. **D** Colony formation assay was conducted to evaluate cell proliferation. Data are presented as mean ± standard deviation ($N = 3$ independent biological replicates). $^{*}p < 0.05$, $^{**}p < 0.01$. Data comparations in (**A**–**D**) were analyzed using two-way ANOVA, followed by Tukey's multiple comparisons test. CAF Cancer-associated fibroblast, EVs extracellular vesicles, NF normal fibroblasts, PCNA proliferating cell nuclear antigen, SMURF2 SMAD-specific E3 ubiquitin protein ligase 2.

through its regulation of downstream target genes[50,51]. Previous studies have identified a binding relationship between TCF12 and the transcription factor *FOXH1*[52]. Our findings confirmed that TCF12 binds to the *FOXH1* promoter, enhancing *FOXH1* expression in HCC cells. FOXC1, like other FOX family proteins, plays a significant oncogenic role in HCC. For instance, FOXC1 has been shown to induce proliferation, invasion, and migration in HCC, with patients expressing FOXC1 having poorer prognosis and more advanced disease stages[53,54]. Similarly, FOXH1 is overexpressed in HCC and has been reported to promote cell growth, migration, and invasion[36]. Consistent with these findings, our study showed that *FOXH1* is highly expressed in HCC cells, and its expression is further enhanced by *SMURF2* overexpression.

Importantly, downregulation of *FOXH1* led to reduced cell viability and inhibition of cell proliferation, suggesting that *FOXH1* is essential for the malignant phenotype of HCC cells. Furthermore, there is evidence suggesting that FOXH1 may may interact with the Wnt/β-catenin signaling pathway, which could be a potential mechanism linking FOXH1 to cancer progression[34,55]. Exploring the connection between FOXH1 and Wnt/β-catenin signaling could be a promising direction for future research. In conclusion, our study indicates that *FOXH1* plays an oncogenic role in

A

Matrix ID	Name	Score	Relative score	Sequence ID	Start	End	Strand	Predicted sequence
MA1648.2	MA1648.2.TCF12	8.965327	0.9024829351169288	NC_000008.11:c144477849-144475849	1637	1643	+	CAGCTGC

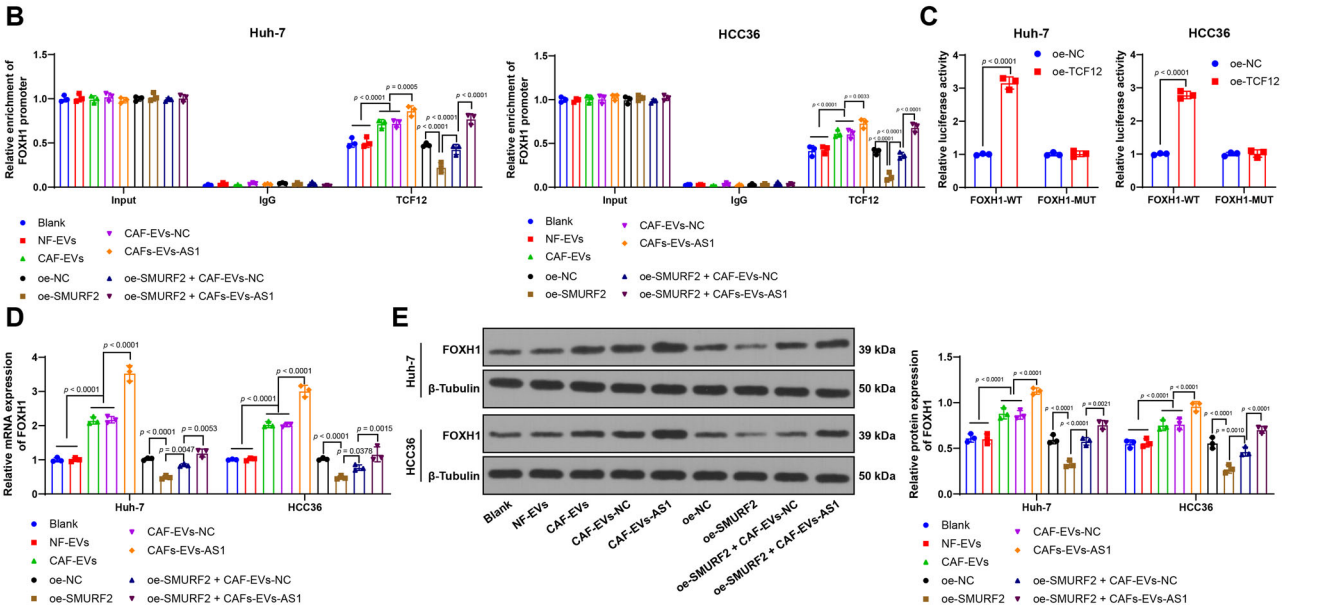

Fig. 7 | TCF12 binds to the *FOXH1* promoter to promote *FOXH1* expression. **A** The JASPAR database was used to predict the binding sites of TCF12 on the *FOXH1* promoter. **B** ChIP assay was performed to analyze the enrichment of TCF12 on the *FOXH1* promoter. **C** Dual-luciferase reporter assay was used to detect the binding relationship between TCF12 and the *FOXH1* promoter sequence. **D**, **E** qRT-PCR and Western blot assay were performed to measure the expression of *FOXH1* in cells with different treatments. Data are presented as mean ± standard deviation ($N = 3$ independent biological replicates). $^{**}p < 0.01$. Data comparations were compared using two-way ANOVA, followed by Tukey's multiple comparisons test. CAF Cancer-associated fibroblast, EVs extracellular vesicles, NF normal fibroblasts, TCF12 Transcription factor 12, SMURF2 SMAD-specific E3 ubiquitin protein ligase 2, FOXH1 Forkhead box H1.

HCC, and its knockdown can alleviate the malignant proliferation of HCC cells.

There are several limitations to our current study. Firstly, the interactions and mechanisms among various cells within the tumor microenvironment are highly complex. In this study, we focused on just one potential mechanism, leaving many other interactions unexplored. Secondly, while we demonstrated the regulatory role of *MAPKAPK5-AS1*, its mechanisms of action may extend beyond the ceRNA pathway and could involve other processes, such as m6A modifications, which require further investigation. Thirdly, due to constraints in experimental conditions and funding, we were unable to perform in vivo experiments using HCC36 cells, which would have provided more comprehensive insights. Finally, we did not explore whether other E3 ubiquitin ligases may also play a role in TCF12 degradation, nor did we investigate the possibility that *MAPKAPK5-AS1* might regulate TCF12 expression through alternative mechanisms.

In future studies, we aim to design more comprehensive experiments to delve deeper into the mechanisms of interaction between various cells within the TEM of HCC. Additionally, we plan to further explore downstream mechanisms of *MAPKAPK5-AS1* and examine the potential involvement of other E3 ubiquitin ligases in TCF12 regulation. These investigations will provide valuable insights and directions for therapeutic approaches to HCC.

In conclusion, our study identified that CAF-EVs carrying *MAPKAPK5-AS1* enter HCC cells, competitively bind to SMURF2, stabilize TCF12 expression, and subsequently promote *FOXH1* expression, facilitating the malignant proliferation of HCC cells. This discovery presents a target for HCC treatment and opens up avenues for therapeutic development.

Materials and methods

Ethics statement

This study was approved by the Ethics Committee of Jinhua Municipal Central Hospital, and all ethical regulations relevant to human research participants were followed. The written informed consent was obtained from all patients. All animal experiments were approved by the Ethics Committee of HANGZHOU HIBIO TECHNOLOGY CO., LTD. The care and use of animals followed the guidelines established by the National Institutes of Health Guide for the Care and Use of Laboratory Animals[56], and we adhered to all ethical regulations related to animal use during the experimental process.

Isolation of NFs and CAFs

CAFs and NFs were isolated from fresh HCC tissues and adjacent healthy tissues (located >10 cm from the tumor infiltration edge) obtained from 10 HCC patients (6 males, 4 females, aged 55–76 years) who had not undergone radiotherapy or chemotherapy prior to surgery. Tissues were processed within 1 h of collection. After rinsing with 75% alcohol and D-Hanks buffer to remove residual blood, tissues were minced into small fragments using sterile surgical blades. These fragments were digested in a solution of collagenase (1 mg mL^{-1}, Gibco, Grand Island, NY, USA) and hyaluronidase (0.5 mg mL^{-1}, Sigma-Aldrich, St. Louis, MO, USA) at 37°C for 1 h. The digested mixture was centrifuged at 1000 g for 5 min, and the cell pellet was washed twice with phosphate-buffered saline (PBS) in Dulbecco's modified Eagle medium (DMEM) (Gibco) to eliminate fat and tissue debris.

The remaining tissues were cultured in DMEM supplemented with 15% fetal bovine serum (FBS, Gibco) for 2 days. After removing the non-adherent cells, adherent cells - mainly fibroblasts, macrophages, and epithelial cells—were cultured. Within 3–5 days, macrophages and epithelial

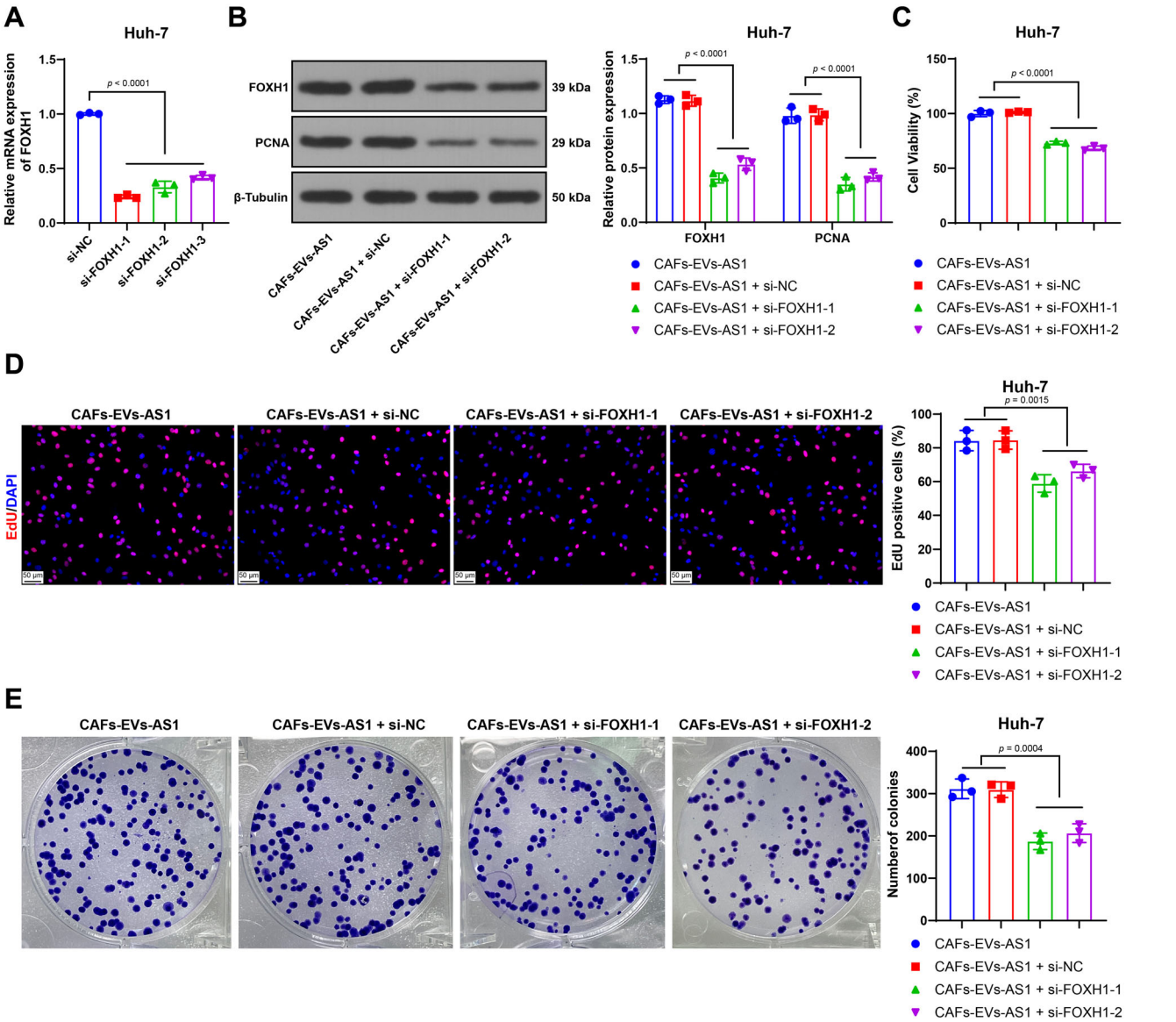

Fig. 8 | Suppression of *FOXH1* partially reverses the promotive effect of CAF-EVs on malignant proliferation of HCC cells. Huh-7 cells were transfected with si-FOXH1 (si-FOXH1-1, si-FOXH1-2, si-FOXH1-3), with si-NC as a control. **A** qRT-PCR was performed to assess the transfection efficiency. Two siRNAs with better knockdown efficiency were selected for further experiments, and co-transfected with CAF-EVs-AS1 containing 100 μg of total protein. **B** Western blot assay was conducted to detect the expression of FOXH1 and PCNA in the cells. **C** Cell viability was assessed using the CCK-8 assay. **D** EdU staining was used to evaluate cell proliferation. **E** Colony formation assay was performed to measure cell proliferation. Data are presented as mean ± standard deviation ($N = 3$ independent biological replicates). $^{**}p < 0.01$. Data comparations in **A**, and **C**–**E** were analyzed using one-way ANOVA, while data comparations in (**B**) were analyzed using two-way ANOVA, followed by Tukey's multiple comparisons test. CAF Cancer-associated fibroblast, EVs extracellular vesicles, FOXH1 Forkhead box H1, PCNA proliferating cell nuclear antigen.

cells underwent apoptosis, leaving only fibroblasts. Fresh medium was replaced every 2–3 days. Primary fibroblasts isolated from tumor tissues were classified as CAFs, while those from normal tissues were designated as NFs. Both CAFs and NFs were maintained in DMEM containing 10% FBS, 1% penicillin, and 1% streptomycin (Gibco) and used for experiments after three passages.

Immunofluorescence characterization of fibroblasts

CAFs and NFs were fixed with 4% paraformaldehyde for 15 min, permeabilized with 0.01% Triton-X-100, and blocked with 2% bovine serum albumin (BSA) for 1 h. Cells were incubated overnight at 4°C with primary antibodies against α-SMA (1:250, ab124964, Abcam, Cambridge, MA, USA), Vimentin (1:250, ab45939, Abcam), keratin (1:200, ab53280, Abcam), and CD31 (1:200, ab32457, Abcam). The following day, cells were incubated at room temperature for 1 h with Alexa Fluor® 647-conjugated secondary antibody (goat anti-rabbit immunoglobulin G, IgG, 1:500, ab150079, Abcam). Nuclei were counterstained with 4',6-diamidino-2-phenylindole (DAPI), and images were acquired using an SP5 confocal microscope (Leica Microsystems, Buffalo Grove, IL, USA).

Establishment of *MAPKAPK5-AS1* overexpression in CAFs

To generate a stable cell line overexpressing *MAPKAPK5-AS1*, the complementary DNA (cDNA) of *MAPKAPK5-AS1* was amplified and subcloned into the lentiviral vector GV248 (Genechem, Shanghai, China). Lentiviruses of overexpression of lncRNA *MAPKAPK5-AS1* (*MAPKAPK5-AS1*) and the corresponding control vector (NC) were synthesized and packaged by Genechem. CAFs with stable overexpression of *MAPKAPK5-AS1* were selected using puromycin (2 μg mL^{-1}).

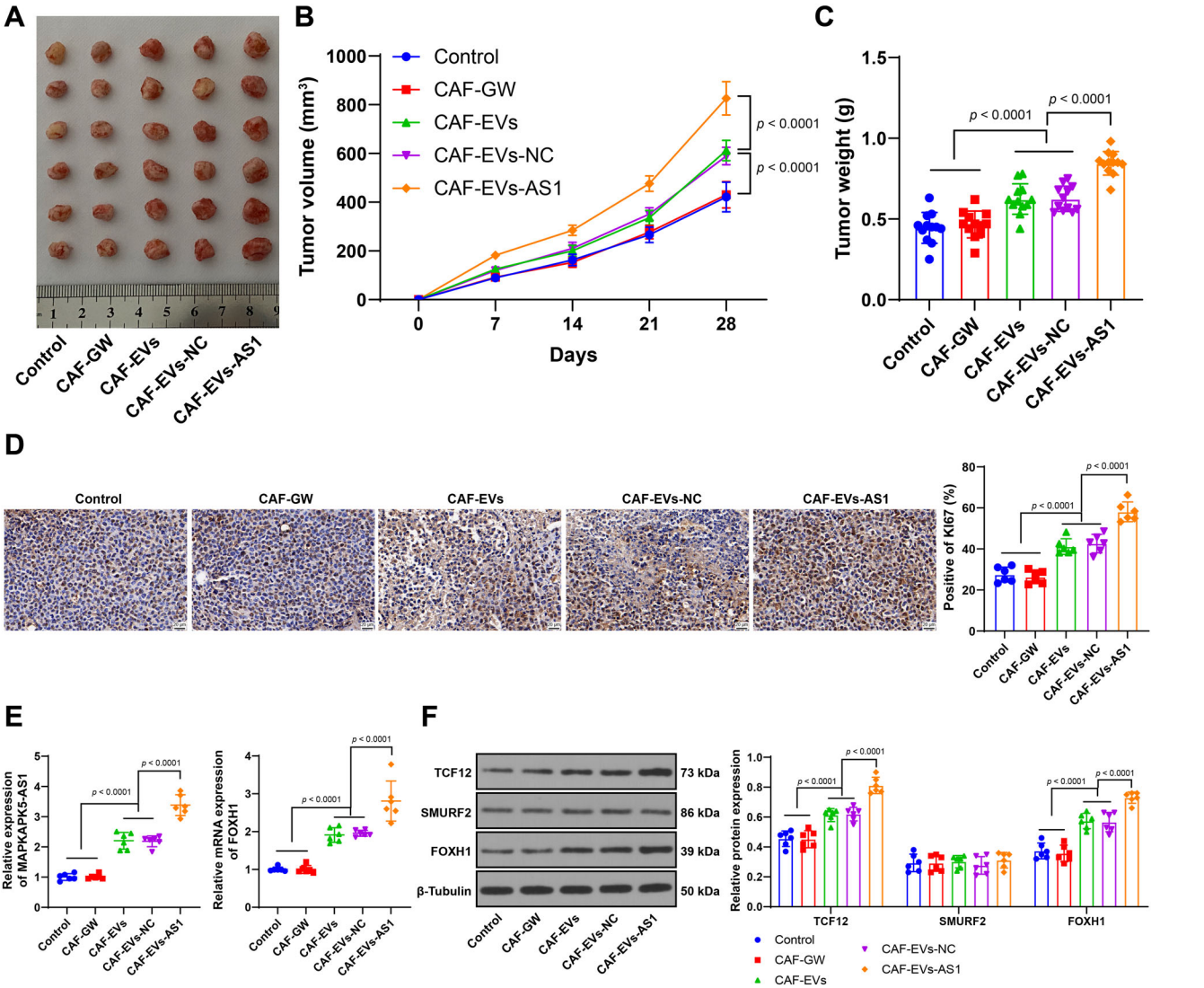

Fig. 9 | CAF-EVs promote HCC growth in vivo. The Huh-7 cells were treated with different CAF-EVs (100 μg of total protein in 50 μL PBS), with equal amounts of CAF-GW treatment as the negative control, and untreated cells as the control group. After 12 h, the cells were washed with PBS to remove excess EVs. The cell suspension was prepared and then injected subcutaneously into the right inguinal area of nude *mice* (2×10^6 cells in 200 μL). Tumors were collected after 28 days. **A** Representative images of tumors from each group. **B** Tumor volume measurement ($n = 12$). **C** Tumor weight ($n = 12$). **D** IHC staining to detect KI67-positive cells in tumors ($n = 6$). **E** qRT-PCR to measure the expression of *MAPKAPK5-AS1* and *FOXH1* in tumors ($n = 6$). **F** Western blot assay to assess the expression of TCF12, SMURF2, and FOXH1 in tumors ($n = 6$). The data are presented as mean ± standard deviation. $^{**}p < 0.01$. Data comparations in **C**–**E** were analyzed using one-way ANOVA, while data comparations in (**B**, **F**) were analyzed using two-way ANOVA, followed by Tukey's multiple comparisons test. CAF Cancer-associated fibroblast, EVs extracellular vesicles, TCF12 Transcription factor 12, SMURF2 SMAD-specific E3 ubiquitin protein ligase 2, FOXH1 Forkhead box H1, GW GW4869.

Briefly, CAFs were seeded in 6-well plates at a density of 2×10^5 cells per well. When cells reached 50%–60% confluence, lentiviral infection was performed using a 50-fold multiplicity of infection (MOI). Polybrene (50 μg mL^{-1}) was added to enhance viral transduction. After 72 h, CAFs were collected, and EVs were isolated from these cells. The resulting EVs were termed CAF-EVs-NC and CAF-EVs-AS1, respectively. Additionally, CAFs were treated with RNase A (Sigma-Aldrich, 2 mg mL^{-1}) or in combination with Triton X-100 (0.1%) for 20 min to confirm the presence of *MAPKAPK5-AS1* in CAF-derived EVs.

Extraction and identification of CAF-EVs and NF-EVs

Equal amounts of CAFs or NFs were cultured in DMEM without FBS for 24 h. The conditioned medium was collected and centrifuged at 2000 g for 30 min to remove dead cells, cell debris, and large EVs. Next, Afterward, the supernatant was treated with a total exosome isolation reagent (4478359, Thermo Fisher Scientific Inc., Waltham, MA, USA) and incubated overnight at 2–8°C. EVs were then isolated via centrifugation at 10,000 g for 60 min, resuspended in PBS, and designated as CAF-EVs or NF-EVs, based on their origin. The protein concentration of the EVs was quantified using a bicinchoninic acid (BCA) assay kit, and this was used as the quantitative standard for EVs.

TEM was utilized to examine the EVs. A total of 10 μg of EVs were placed on a copper grid, fixed with 10 μL of 2.5% glutaraldehyde for 5 min, rinsed with distilled water, stained with 1% uranyl acetate, and air-dried at room temperature for 20 min. EV morphology and particle size were observed using a TEM (JEM-2100, Hitachi, Tokyo, Japan) at 160.0 kV. NTA (Malvern Instruments Ltd., UK) was also used to assess particle size. Western blotting was performed to detect the expression of EV protein markers CD9 (1:1000, ab236630, Abcam), CD63 (1:1000, ab134045, Abcam), and the negative control Calnexin (1:1000, ab22595, Abcam). The EV generation inhibitor GW4869 (10 μM; Sigma-Aldrich) was added to CAFs or NFs, with the conditioned medium labeled as the GW group. Lyophilized PC-3 exosome standards (PC3-EVs) (Abcam, ab239689) were used as a positive control.

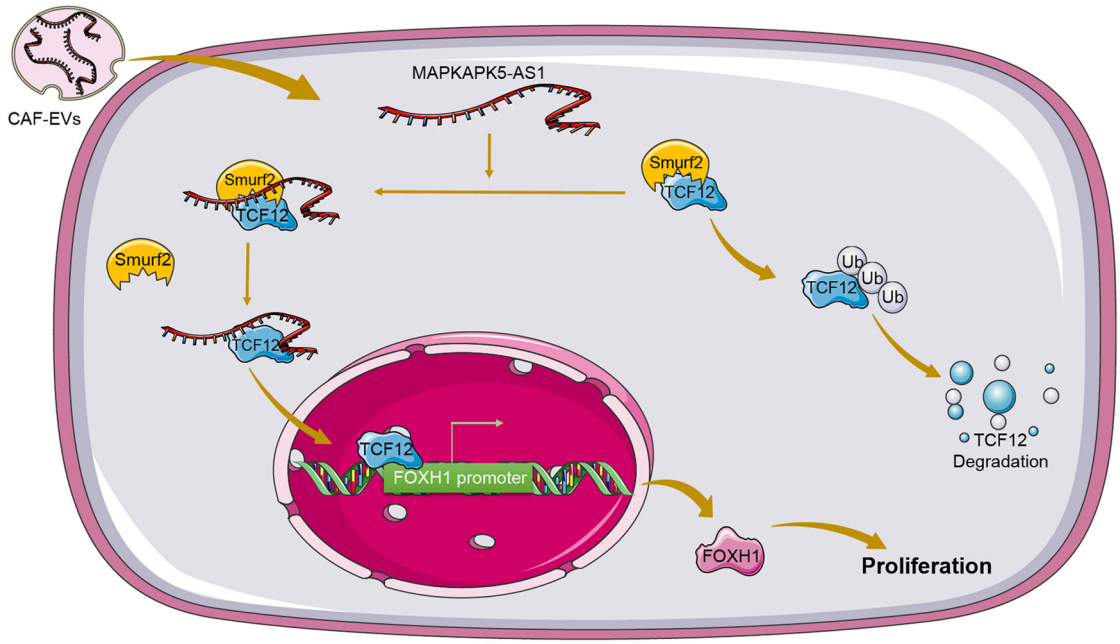

Fig. 10 | CAF-EVs facilitate malignant proliferation of HCC cells by delivering *MAPKAPK5-AS1*, which competitively binds to SMURF2, stabilizes TCF12 expression, and promotes *FOXH1* expression. CAF Cancer-associated fibroblast, EVs extracellular vesicles, TCF12 Transcription factor 12, SMURF2 SMAD-specific E3 ubiquitin protein ligase 2, FOXH1 Forkhead box H1.

Cell culture and treatment

Human HCC cell lines Huh-7 and HCC36 were obtained from the American Type Culture Collection (ATCC; Maryland, MD, USA) and authenticated through short tandem repeat (STR) analysis. Both cell lines were confirmed to be free of mycoplasma contamination. Cells were cultivated in DMEM (Gibco) supplemented with 10% FBS (Gibco), 100 UmL^{-1} penicillin, and 100 μg mL^{-1} streptomycin (Sigma-Aldrich) in a humidified incubator at 37°C with 5% CO_2.

Huh-7 or HCC36 cells were seeded in 6-well plates and treated with NF-EVs or CAF-EVs containing 100 μg of protein (in 50 μL PBS). Equal amounts of NF-GW or CAF-GW were used as negative controls. Transfection of *SMURF2* overexpression vector (oe-SMURF2) or empty vector (GenePharma, Shanghai, China) and three *FOXH1* siRNAs (Guangzhou RiboBio, Guangzhou, China) was carried out using Lipofectamine 3000 (Invitrogen, Carlsbad, CA, USA). Experiments were performed 24 h post-transfection.

Cy3-labeled fluorescence observation

To track the transfer of CAF-EVs-carried lncRNA *MAPKAPK5-AS1*, Cy3-labeled *MAPKAPK5-AS1* (GenePharma) was transfected into CAFs, followed by co-culture with Huh-7 or HCC36 cells in 24-well Transwell chambers for 48 h. Cell skeletons were stained with FITC phalloidin (Yeasen, Shanghai, China). GW4869 was included in the system to inhibit EV release. Internalization of CAF-EVs-carried lncRNA *MAPKAPK5-AS1* was observed using a confocal microscope (Leica Microsystems, Mannheim, Germany).

Subcellular fractionation

Cytoplasmic and nuclear RNA was isolated from Huh-7 and HCC36 cells using cytoplasmic & nuclear RNA purification kits purification kits (Norgen, Thorold, Ontario, Canada) according to the manufacturer's protocol[57]. The expression levels of lncRNA *MAPKAPK5-AS1* were analyzed using qRT-PCR, with glyceraldehyde 3-phosphate dehydrogenase (GAPDH) and U6 serving as controls for cytoplasmic and nuclear RNA, respectively.

CCK-8 assay

Cell viability was evaluated using the CCK-8 assay kit (Nanjing Jiancheng, Jiangsu, China). Cells, subjected to various treatments, were seeded in 96-well plates at a density of 2×10^3 cells per well. Following an overnight incubation, 10 μL of CCK-8 reagent was added to each well, and the plates were incubated for 1 h at 37°C. Absorbance was measured at 450 nm using a Multiskan^{TM} FC microplate spectrophotometer (Thermo Fisher Scientific).

EdU assay

Cell proliferation was assessed using an EdU staining kit (Beyotime, Shanghai, China). Cells were seeded in 12-well plates and incubated at 37°C for 24 h. The cells were then treated with 200 μL of EdU (500 μM) at 37°C for 2 h. Afterward, cells were fixed with 4% paraformaldehyde for 15 min at room temperature and permeabilized with 0.3% Triton X-100 for 10 min. The cells were subsequently stained with 2 μg mL^{-1} Hoechst 33342 (Beyotime) for 30 min at room temperature. EdU-positive cells were visualized and imaged using a fluorescence microscope (Leica Microsystems).

Colony formation assay

Following various treatments, cells were seeded in 6-well plates at 1000 cells per well and incubated at 37°C in a 5% CO_2 atmosphere for 14 days. Cells were then fixed with 4% paraformaldehyde (700 μL per well, Sigma-Aldrich) for 20 min and washed twice with PBS. After washing, the cells were stained with 1% crystal violet (700 μL per well, Sigma-Aldrich) at room temperature for 30 min, followed by PBS washing and air drying. Colony formation was observed and imaged under an Olympus microscope, and the colonies were quantified using J software (National Institutes of Health, Bethesda, Maryland, USA).

qRT-PCR

Total RNA was extracted from cells and tumor tissues using TRIzol reagent (Invitrogen). cDNA was synthesized using the M-MLV reverse transcriptase kit (Invitrogen) according to the manufacturer's protocol. qRT-PCR was performed using the SYBR Premix Ex Taq kit (Takara, Dalian, China), and the relative gene expression levels were calculated using the

$2^{-\Delta\Delta CT}$ method[58]. GAPDH and U6 were used as internal reference genes. The primer sequences are provided in Supplementary Table 1.

Western blot assay

Total protein was isolated from tissues and cells using radioimmunoprecipitation assay (RIPA) buffer (Beyotime) on ice, followed by quantification using the BCA assay kit (Millipore). Protein samples were mixed with loading buffer and heated in boiling water. Equal amounts of protein were separated by sodium dodecyl sulfate polyacrylamide gel electrophoresis (SDS-PAGE), transferred onto polyvinylidene fluoride membranes (Millipore), and blocked with 5% non-fat milk at room temperature for 2 h. The membranes were incubated overnight at 4°C with primary antibodies against SMURF2 (1:2000, MA5-42771, Invitrogen), TCF12 (1:2000, ab245540, Abcam), FOXH1 (1:1000, ab229241, Abcam), PCNA (1:2000, ab92552, Abcam), and β-Tubulin (1:500, ab6046, Abcam). The following day, the membranes were incubated with secondary IgG antibodies (1:3000, ab6721, Abcam) at room temperature for 2 h. Protein signals were detected using an enhanced chemiluminescence detection reagent (Sangon, Shanghai, China).

Bioinformatics analysis

The interaction between *MAPKAPK5-AS1* and TCF12 was analyzed using the RPISeq database (http://pridb.gdcb.iastate.edu/RPISeq/index.html)[59]. The subcellular localization of *MAPKAPK5-AS1* was predicted using the lncATLAS database (https://lncatlas.crg.eu/?tdsourcetag=s_pcqq_aiomsg)[60]. The binding sites between TCF12 and FOXH1 promoter sequences were predicted using the JASPAR database (https://jaspar.elixir.no/)[61].

RNA pull-down assay

Total RNA was extracted from cells using TRIzol (TaKaRa, Beijing, China), and reverse transcription and amplification were performed via qPCR using primers containing a T7 promoter sequence targeting *MAPKAPK5-AS1* (NR_152605.1) and the antisense of *MAPKAPK5-AS1*. Following purification, the amplified products were transcribed into RNA in vitro using the Transcript Aid T7 High Yield Transcription Kit (Thermo Fisher Scientific). Subsequently, biotinylated RNA was synthesized using the Pierce™ RNA 3' End Biotinylation Kit (Thermo Fisher Scientific). Cells were lysed using RIPA lysis buffer. Biotin-labeled lncRNA *MAPKAPK5-AS1* was bound to streptavidin magnetic beads and incubated with cell lysates overnight at 4°C. The RNA-protein complexes were washed and eluted, and the associated proteins were analyzed by Western blot.

Co-Immunoprecipitation (Co-IP)

Equal amounts of protein were incubated with the primary antibody SMURF2 (1:1000, MA5-42771, Invitrogen) overnight at 4°C. This was followed by incubation with protein A agarose beads (Pierce Biotechnology, Waltham, MA, USA) overnight at 4°C. The samples were then washed with IP lysis buffer and subjected to SDS-PAGE. After transfer, the membranes were probed with TCF12 (1:1000, ab245338, Abcam) or anti-ubiquitin antibody (1:2000, ab134953, Abcam) and analyzed by Western blot.

ChIP

HCC cells were fixed with 1% formaldehyde for 10 min to crosslink proteins to DNA, followed by lysis of cell membrane and nuclei. Chromatin was fragmented by sonication to produce smaller DNA fragments. The chromatin suspension was diluted 1:5 in dilution buffer, and 5% of the original volume was set aside as an untreated control sample (Input). The remaining chromatin was split for immunoprecipitation, with one part incubated with TCF12 antibody (1:1000, ab245338, Abcam) and the other with normal rabbit IgG antibody. Both were incubated overnight at 4°C on a shaker. Protein A/G magnetic beads were used to capture the immunoprecipitated complexes, and the samples were then washed and de-crosslinked by incubation overnight at 65°C. DNA was purified using a PCR product extraction kit (Qiagen, Hilden, Germany). The total DNA used as input, while the immunoprecipitated DNA was used as a template for further analysis. The primers used for amplification are provided in Supplementary Table 1.

Dual-luciferase reporter assay

The FOXH1 promoter sequence containing the TCF12 binding site was cloned into a luciferase reporter vector to create the FOXH1-WT construct. A mutant version of the TCF12 binding site in the FOXH1 promoter sequence was also generated and cloned into the luciferase reporter vector (FOXH1-MUT) following the manufacturer's protocol (RiboBio). These reporter vectors were co-transfected into cells using Lipofectamine 3000, along with either an overexpression TCF12 vector (oe-TCF12) or empty vector (oe-NC). After 48 h, luciferase activity was measured using the dual-glo luciferase assay system (Promega, Madison, WI, USA) and a luminometer. Each experiment was repeated three times to ensure reproducibility.

Tumor xenograft in nude mice

Male BALB/c nude *mice* (4–6 weeks old; $n = 12$ per group) were obtained from Beijing Vital River Laboratory Animal Technology (Beijing, China) and housed under standard conditions with a 12 h light-dark cycle, with free access to food and water. A total of 1.5×10^6 Huh-7 cells were cultured in media and treated with different CAF-EVs (100 μg of total protein in 50 μL PBS)[62]. An equivalent amount of CAF-GW treatment served as the negative control, with untreated cells as the baseline control group. After 12 h of treatment, Huh-7 cells were washed with PBS to remove excess EVs and prepared as a cell suspension. Based on the following treatments, *Mice* were numbered according to their body weight and assigned into 5 groups using random number method (12 *mice* per group): Control group, CAF-GW group, CAF-EVs group, CAF-EVs-NC group, and CAF-EVs-AS1 group. Each *mouse* was subcutaneously injected with 2×10^6 cells in 200 μL of suspension into the right inguinal region. Tumor volume was measured weekly using the formula $V = 0.5 \times L \times W^2$ (length × width). After 4 weeks, the *mice* were euthanized, or the humane endpoint was reached when the maximum tumor diameter reached ≥15 mm. No unexpected deaths occurred, and all *mice* reached the experimental endpoint. Tumors were excised and weighed. Samples from 6 *mice* per group were reserved for immunohistochemical staining, while the remaining 6 samples were used for qRT-PCR or Western blot assays.

Immunohistochemistry (IHC)

Tumor tissues were fixed in 4% paraformaldehyde, embedded in paraffin, and sectioned at 4 μm thickness. Paraffin sections were deparaffinized in xylene, dehydrated through a series of graded ethanol solutions (100%, 95%, 90%, and 85%), and rehydrated. Antigen retrieval was performed using citrate buffer antigen retrieval solution (pH 6). Sections were incubated with KI67 antibody (1:200, ab15580, Abcam) to block endogenous peroxidase and to seal the sections. After overnight incubation at 4°C, sections were treated with a polymerized horseradish peroxidase-conjugated secondary antibody (1:3000, ab6721, Abcam) at 25°C for 2 h. The reaction product was developed with 3,3'-diaminobenzidine tetrahydrochloride (DAB) and counterstained with hematoxylin. Finally, the stained sections were examined under a Nikon ECLIPSE Ts2R microscope, and the results were analyzed by a blinded researcher.

Statistics and reproducibility

All statistical analyses were conducted using SPSS 21.0 statistical software (SPSS, IBM, Armonk, NY, USA) and GraphPad Prism 8.0 software (GraphPad Software Inc., San Diego, CA, USA). Data were first tested for normality and homogeneity of variance, confirming a normal distribution and homogeneity of variance. Comparisons between two groups were performed using the *t*-test, while one-way or two-way analysis of variance (ANOVA) was used for comparisons among multiple groups, followed by Tukey's multiple comparisons test for post-hoc analysis. All *p*-values were two-tailed, with $p < 0.05$ considered statistically significant and $p < 0.01$ considered highly statistically significant. Cell experiments were

independently repeated three times, while animal experiments consisted of 12 or 6 *mice* per group. The mean and standard deviation were calculated.

Data availability

All data are available from the corresponding authors upon reasonable request and all numerical source data can be found in Supplementary Data.

Received: 19 May 2024; Accepted: 18 December 2024;
Published online: 30 December 2024

References

1. Chidambaranathan-Reghupaty, S., Fisher, P. B. & Sarkar, D. Hepatocellular carcinoma (HCC): epidemiology, etiology and molecular classification. *Adv. Cancer Res.* **149**, 1–61 (2021).
2. Forner, A., Reig, M. & Bruix, J. Hepatocellular carcinoma. *Lancet* **391**, 1301–1314 (2018).
3. Yang, J. D. et al. A global view of hepatocellular carcinoma: trends, risk, prevention and management. *Nat. Rev. Gastroenterol. Hepatol.* **16**, 589–604 (2019).
4. Huang, A., Yang, X. R., Chung, W. Y., Dennison, A. R. & Zhou, J. Targeted therapy for hepatocellular carcinoma. *Signal Transduct. Target Ther.* **5**, 146 (2020).
5. Zulaziz, N., Chai, S. J. & Lim, K. P. The origins, roles and therapies of cancer associated fibroblast in liver cancer. *Front Oncol.* **13**, 1151373 (2023).
6. Ying, F., Chan, M. S. M. & Lee, T. K. W. Cancer-associated fibroblasts in hepatocellular carcinoma and cholangiocarcinoma. *Cell Mol. Gastroenterol. Hepatol.* **15**, 985–999 (2023).
7. Abels, E. R. & Breakefield, X. O. Introduction to extracellular vesicles: biogenesis, RNA cargo selection, content, release, and uptake. *Cell Mol. Neurobiol.* **36**, 301–312 (2016).
8. Clancy, J. W. & D'Souza-schorey, C. tumor-derived extracellular vesicles: multifunctional entities in the tumor microenvironment. *Annu Rev. Pathol.* **18**, 205–229 (2023).
9. Zhou, Y. et al. Hepatocellular carcinoma-derived exosomal miRNA-21 contributes to tumor progression by converting hepatocyte stellate cells to cancer-associated fibroblasts. *J. Exp. Clin. Cancer Res.* **37**, 324 (2018).
10. Yugawa, K. et al. Cancer-associated fibroblasts promote hepatocellular carcinoma progression through downregulation of exosomal miR-150-3p. *Eur. J. Surg. Oncol.* **47**, 384–393 (2021).
11. Chi, Y., Wang, D., Wang, J., Yu, W. & Yang, J. Long non-coding RNA in the pathogenesis of cancers. *Cells* **8**, 1015 (2019).
12. Zheng, R. et al. Long noncoding RNA lnc-LOC645166 promotes adriamycin resistance via NF-kappaB/GATA3 axis in breast cancer. *Aging (Albany NY)* **12**, 8893–8912 (2020).
13. Zhang, C., Chen, D., Gu, Y., Wang, T. & Wang, C. Effects of LncRNA GAS5/miR-137 general anesthesia on cognitive function by TCF4 inflammatory bodies in patients undergoing lumbar spinal canal decompression. *Med. (Baltim.)* **101**, e31880 (2022).
14. Dong, Q. et al. LncRNA GAS5 suppresses ovarian cancer progression by targeting the miR-96-5p/PTEN axis. *Ann. Transl. Med.* **9**, 1770 (2021).
15. Ji, J. et al. Long non-coding RNA Lnc-Tim3 exacerbates CD8 T cell exhaustion via binding to Tim-3 and inducing nuclear translocation of Bat3 in HCC. *Cell Death Dis.* **9**, 478 (2018).
16. Wang, Z. et al. Long noncoding RNA MyD88 functions as a promising diagnostic biomarker in hepatocellular carcinoma. *Front Endocrinol. (Lausanne)* **14**, 938102 (2023).
17. Wang, L. et al. Long non-coding RNA MAPKAPK5-AS1/PLAGL2/HIF-1alpha signaling loop promotes hepatocellular carcinoma progression. *J. Exp. Clin. Cancer Res.* **40**, 72 (2021).
18. Peng, Z., Ouyang, X., Wang, Y. & Fan, Q. MAPKAPK5-AS1 drives the progression of hepatocellular carcinoma via regulating miR-429/ZEB1 axis. *BMC Mol. Cell Biol.* **23**, 21 (2022).
19. Lv, E., Sheng, J., Yu, C., Rao, D. & Huang, W. Long noncoding RNA MAPKAPK5-AS1 promotes metastasis through regulation miR-376b-5p/ECT2 axis in hepatocellular carcinoma. *Dig. Liver Dis.* **55**, 945–954 (2023).
20. Shoucair, I., Weber Mello, F., Jabalee, J., Maleki, S. & Garnis, C. The role of cancer-associated fibroblasts and extracellular vesicles in tumorigenesis. *Int. J. Mol. Sci.* **21**, 6837 (2020).
21. Fu, L., Cui, C. P., Zhang, X. & Zhang, L. The functions and regulation of Smurfs in cancers. *Semin Cancer Biol.* **67**, 102–116 (2020).
22. Koganti, P., Levy-Cohen, G. & Blank, M. Smurfs in protein homeostasis, signaling, and cancer. *Front Oncol.* **8**, 295 (2018).
23. Han, M. et al. SMURF2 facilitates ubiquitin-mediated degradation of ID2 to attenuate lung cancer cell proliferation. *Int. J. Biol. Sci.* **19**, 3324–3340 (2023).
24. Pi, Y. et al. Loss of SMURF2 expression enhances RACK1 stability and promotes ovarian cancer progression. *Cell Death Differ.* **30**, 2382–2392 (2023).
25. Song, D., Li, S., Ning, L., Zhang, S. & Cai, Y. Smurf2 suppresses the metastasis of hepatocellular carcinoma via ubiquitin degradation of Smad2. *Open Med. (Wars.)* **17**, 384–396 (2022).
26. Gao, S., Bian, T., Zhang, Y., Su, M. & Liu, Y. TCF12 overexpression as a poor prognostic factor in ovarian cancer. *Pathol. Res. Pr.* **215**, 152527 (2019).
27. Gao, S., Bian, T., Su, M., Liu, Y. & Zhang, Y. miR-26a inhibits ovarian cancer cell proliferation, migration and invasion by targeting TCF12. *Oncol. Rep.* **43**, 368–374 (2020).
28. Yang, J. et al. TCF12 promotes the tumorigenesis and metastasis of hepatocellular carcinoma via upregulation of CXCR4 expression. *Theranostics* **9**, 5810–5827 (2019).
29. Chen, X. et al. CircUSP10 promotes liver cancer progression by regulating miR-211-5p/TCF12/EMT signaling pathway. *Heliyon* **9**, e20649 (2023).
30. Bach, D. H. et al. The dominant role of forkhead box proteins in cancer. *Int. J. Mol. Sci.* **19**, 3279 (2018).
31. O'Regan, R. M. & Nahta, R. Targeting forkhead box M1 transcription factor in breast cancer. *Biochem Pharm.* **154**, 407–413 (2018).
32. Liu, Y., Zhang, L., Meng, Y. & Huang, L. Benzyl isothiocyanate inhibits breast cancer cell tumorigenesis via repression of the FoxH1-mediated Wnt/beta-catenin pathway. *Int J. Clin. Exp. Med.* **8**, 17601–17611 (2015).
33. Kim, C. G. et al. Role of forkhead box class O proteins in cancer progression and metastasis. *Semin. Cancer Biol.* **50**, 142–151 (2018).
34. Zhang, J. et al. FOXH1 promotes lung cancer progression by activating the Wnt/beta-catenin signaling pathway. *Cancer Cell Int* **21**, 293 (2021).
35. Lamouille, S., Xu, J. & Derynck, R. Molecular mechanisms of epithelial-mesenchymal transition. *Nat. Rev. Mol. Cell Biol.* **15**, 178–196 (2014).
36. Ouyang, X. et al. A comprehensive analysis of FOX family in HCC and experimental evidence to support the oncogenic role of FOXH1. *Aging (Albany NY)* **14**, 2268–2286 (2022).
37. Zhao, D. et al. CircN4bp1 facilitates sepsis-induced acute respiratory distress syndrome through mediating macrophage polarization via the miR-138-5p/EZH2 Axis. *Med. Inflamm.* **2021**, 7858746 (2021).
38. Tao, L., Li, D., Mu, S., Tian, G. & Yan, G. LncRNA MAPKAPK5_AS1 facilitates cell proliferation in hepatitis B virus -related hepatocellular carcinoma. *Lab Invest.* **102**, 494–504 (2022).
39. Huang, T. et al. A positive feedback between PDIA3P1 and OCT4 promotes the cancer stem cell properties of esophageal squamous cell carcinoma. *Cell Commun. Signal* **22**, 60 (2024).
40. Chen, C., Wang, Z., Ding, Y. & Qin, Y. Tumor microenvironment-mediated immune evasion in hepatocellular carcinoma. *Front Immunol.* **14**, 1133308 (2023).

41. Krance, S. H. et al. The complement cascade in Alzheimer's disease: a systematic review and meta-analysis. *Mol. Psychiatry* **26**, 5532–5541 (2021).
42. Xu, H. et al. Cancer associated fibroblast-derived CCL5 promotes hepatocellular carcinoma metastasis through activating HIF1alpha/ZEB1 axis. *Cell Death Dis.* **13**, 478 (2022).
43. Naito, Y., Yoshioka, Y. & Ochiya, T. Intercellular crosstalk between cancer cells and cancer-associated fibroblasts via extracellular vesicles. *Cancer Cell Int.* **22**, 367 (2022).
44. Yang, J. et al. Integrated analysis of an lncRNA-associated ceRNA network reveals potential biomarkers for hepatocellular carcinoma. *J. Comput. Biol.* **28**, 330–344 (2021).
45. Shi, Y. et al. The role of ceRNA-mediated diagnosis and therapy in hepatocellular carcinoma. *Hereditas* **158**, 44 (2021).
46. Zhang, W. L., Zhang, J. H., Wu, X. Z., Yan, T. & Lv, W. miR-15b promotes epithelial-mesenchymal transition by inhibiting SMURF2 in pancreatic cancer. *Int J. Oncol.* **47**, 1043–1053 (2015).
47. Afaloniati, H. et al. Romidepsin hepatocellular carcinoma suppression in mice is associated with deregulated gene expression of bone morphogenetic protein and Notch signaling pathway components. *Mol. Biol. Rep.* **48**, 551–562 (2021).
48. Chaudhary, K. R. et al. Smurf2 inhibition enhances chemotherapy and radiation sensitivity in non-small-cell lung cancer. *Sci. Rep.* **12**, 10140 (2022).
49. Verga-Gerard, A. et al. Hepatitis C virus/human interactome identifies SMURF2 and the viral protease as critical elements for the control of TGF-beta signaling. *FASEB J.* **27**, 4027–4040 (2013).
50. Wang, Z. et al. LncRNA EMX2OS, regulated by TCF12, interacts with FUS to regulate the proliferation, migration and invasion of prostate cancer cells through the cGMP-PKG signaling pathway. *Onco Targets Ther.* **13**, 7045–7056 (2020).
51. Tian, Y. et al. TCF12 Activates TGFB2 expression to promote the malignant progression of melanoma. *Cancers (Basel)* **15**, 4505 (2023).
52. Yoon, S. J., Wills, A. E., Chuong, E., Gupta, R. & Baker, J. C. HEB and E2A function as SMAD/FOXH1 cofactors. *Genes Dev.* **25**, 1654–1661 (2011).
53. Xu, Z. et al. Comprehensive analysis of FOXM1 immune infiltrates, m6a, glycolysis and ceRNA network in human hepatocellular carcinoma. *Front Immunol.* **14**, 1138524 (2023).
54. Lin, Z. et al. FOXC1 promotes HCC proliferation and metastasis by upregulating DNMT3B to induce DNA Hypermethylation of CTH promoter. *J. Exp. Clin. Cancer Res.* **40**, 50 (2021).
55. He, Q. et al. Wnt3a suppresses Wnt/beta-catenin signaling and cancer cell proliferation following serum deprivation. *Exp. Cell Res.* **341**, 32–41 (2016).
56. National Research Council (US). *Guide for the Care and Use of Laboratory Animals The National Academies Collection: Reports funded by National Institutes of Health* 8th edn (The National Academies Press, 2011).
57. Xu, J. et al. LncRNA BBOX1-AS1 upregulates HOXC6 expression through miR-361-3p and HuR to drive cervical cancer progression. *Cell Prolif.* **53**, e12823 (2020).
58. Livak, K. J. & Schmittgen, T. D. Analysis of relative gene expression data using real-time quantitative PCR and the 2(-Delta Delta C(T)) Method. *Methods* **25**, 402–408 (2001).
59. Muppirala, U. K., Honavar, V. G. & Dobbs, D. Predicting RNA-protein interactions using only sequence information. *BMC Bioinforma.* **12**, 489 (2011).
60. Mas-Ponte, D. et al. LncATLAS database for subcellular localization of long noncoding RNAs. *RNA* **23**, 1080–1087 (2017).
61. Rauluseviciute, I. et al. JASPAR 2024: 20th anniversary of the open-access database of transcription factor binding profiles. *Nucleic Acids Res.* **52**, D174–D182 (2024).
62. Chen, X. et al. Exosome-mediated transfer of miR-93-5p from cancer-associated fibroblasts confer radioresistance in colorectal cancer cells by downregulating FOXA1 and upregulating TGFB3. *J. Exp. Clin. Cancer Res.* **39**, 65 (2020).

Acknowledgements

This study was supported by the Zhejiang Province Traditional Chinese Medicine Science and Technology Plan Project Research Fund Project (Grant Number 2022ZB373).

Author contributions

X.B.W., L.S. and J.M.L. contributed to the study's design and manuscript writing. Y.L.Z., Y.P.C. and X.X.Y. performed the experiments. J.M.L. analyzed and interpreted the data. X.B.W. supervised the study and secured the funding. L.S. wrote the manuscript.

Competing interests

The authors declare no competing interests.

Additional information

Supplementary information The online version contains supplementary material available at https://doi.org/10.1038/s42003-024-07428-3.

Correspondence and requests for materials should be addressed to Xiaobo Wang.

Peer review information *Communications Biology* thanks the anonymous reviewers for their contribution to the peer review of this work. Primary Handling Editors: Kaliya Georgieva. [A peer review file is available].